

# Numerical Study of Airfoils Aerodynamic Performance in Heavy Rain Environment

M. Ismail, Cao Yihua, Zhao Ming, Abu Bakar

**Abstract**—Heavy rainfall greatly affects the aerodynamic performance of the aircraft. There are many accidents of aircraft caused by aerodynamic efficiency degradation by heavy rain.

In this Paper we have studied the heavy rain effects on the aerodynamic efficiency of cambered NACA 64-210 and symmetric NACA 0012 airfoils. Our results show significant increase in drag and decrease in lift. We used preprocessing software gridgen for creation of geometry and mesh, used fluent as solver and techplot as postprocessor. Discrete phase modeling called DPM is used to model the rain particles using two phase flow approach. The rain particles are assumed to be inert.

Both airfoils showed significant decrease in lift and increase in drag in simulated rain environment. The most significant difference between these two airfoils was the NACA 64-210 more sensitivity than NACA 0012 to liquid water content (LWC). We believe that the results showed in this paper will be useful for the designer of the commercial aircrafts and UAVs, and will be helpful for training of the pilots to control the airplanes in heavy rain

**Keywords**—airfoil, discrete phase modeling, heavy rain, Reynolds number

## I. INTRODUCTION

HEAVY rain effects on aerodynamic efficiency has been the cause of many aircraft accidents for both transport and general aviation airplanes. Heavy rain rate of 1800mm/h may cause the 30% decrease in lift and 20% increase in drag, also affecting the stall angle, stall speed and maneuverability [1].

These effects cause the reduction in lift, increase in drag and decrease in stall angle. All these factors affect the flight safety, aircraft maneuverability and control.

Meteorologist and aviation communities have been interested to rain associated with thunder storms for many years. LWC (liquid water content) and rain fall rate have been characterized as parameters to express the rain fall. Rainfall rate is the rate at which rain falls on ground and is often measured in unit of mm/h or inch/hr. The LWC is the liquid water content of the air usually expressed in gram per cubic meter ( $\text{g}/\text{m}^3$ ) of air. The relationship between LWC and rain rate R is dependent on the type of storm and rain [2]-[3].

Ismail M. is PhD student in Beijing Aeronautics and Astronautics University, Beijing, China (phone: +86-1364-131-2343; e-mail: ismailbaila@gmail.com).

Yihua C. is working as Professor in Beijing Aeronautics and Astronautics University, Beijing, China (phone: +86-1368-149-1896; e-mail: yihuacaocs@yahoo.com.cn).

Ming Z. is PhD student in Beijing Aeronautics and Astronautics University, Beijing, China (phone: +86-1381-181-4671; e-mail: zmbuaa@163.com).

Bakar A. is MS student in North Western Polytechnical University, Xian, China.

The earliest analytical work on the effects of rain on aerodynamic performance has been done by Rhode in 1941[4]. He showed in his analysis that for the aircraft DC -3 in heavy rain with LWC of  $50 \text{ g}/\text{m}^3$ , the drag increased and caused the 18 % decrease in the true airspeed of aircraft but his study did not seem to be safety concern for the aircraft. In 1983 Haines and Luers [5]-[7] published two articles about heavy rain penalties on aircraft. Their work showed that the heavy rain causes the roughening of wing which becomes the source of decrement of the aerodynamic efficiency which include causes the decrement install angle and the decrement in maximum lift up to 30%.

In 1994 and 1995, Valentine and Decker [8]-[10] conducted a number of simulations to study the aerodynamic performance. They were successful in simulating the rain phenomenon numerically and achieved the degradation of the aerodynamic performance, increase in drag and decrease in lift in their work.

Experimental work done in past showed that the airfoil & wing in heavy rain may subject to decrease in lift, increase in drag, and decrease in stall angle [11]-[17]. In the previous research, researchers identified different phenomenon contributing to aerodynamic efficiency degradation, these include the roughening of the airfoil surface due to the presence of an uneven water film, the decrement in airfoil momentum due to collision of rain particles and the loss of boundary-layer air momentum through the acceleration of splashed-back droplets.

Two approaches are commonly used to model fluid-particle flows i.e. the Eulerian (two fluids) model and Lagrangian (tracking) model. In Eulerian model the particle and fluid phases as are both treated as continuous and for each flow the appropriate conservation equations are solved. In Eulerian approach the phases exchange, mass, momentum, and energy and their mass momentum and energy are included as source terms in the appropriate conservation equations. This model is better and easy to implement for particles of uniform size. In Lagrangian approach a set of Eulerian conservation equations are solved for the continuous fluid phase, then Lagrangian equations of motion are used to determine particle trajectories. In a one-way coupled model it is assumed that the fluid phase influences the particle motion, but the presence of particles does not affect fluid motion. In a two way coupled model both the fluid and particles phases may exchange momentum, mass and energy if applicable between them. To account for the influence of particles on the fluid phase, source terms are added to the fluid conservation equations.

Two approaches are used in Lagrangian two-way coupled models. The first is non-iterative transient scheme in which

particle and fluid flow fields are considered simultaneously and the second is iterative particle-source-in-cell method, in which fluid and particle fields are considered separately and updated iteratively until a stationary solution is reached. Calarese and Hankey [18] implemented the two-way coupled Eulerian scheme to study the rain effects on the aerodynamic performance of a NACA 0012 airfoil for the two limiting cases of very fine and very coarse rain. For very fine rain, increase in lift and drag were predicted as a result of effective increase in fluid density, while no appreciable change in airfoil aerodynamic performance for coarse rain is observed in their research.

In our numerical study we implemented two-way coupled Lagrangian approach to study heavy rain effects on the aerodynamic performance of cambered NACA 64-210 and symmetric NACA 0012 airfoils. We used compressible, turbulent air flow field with Lagrangian equations of motion to track inert rain particles through the air flow field. Raindrop impacts on the airfoil and some of them are splashed back. We assume that rain particles are non-interacting. The assumption of non interacting droplets is justified by Bilanin's [19]. According to him even for extremely high rainfall of 1872 mm/h and for an average raindrop diameter of 4 mm, the mean distance between raindrops will be of the order of 7 cm or 17.5 times the drop diameter. Thus raindrop collisions should not occur frequently so we can neglect the collision of the particles in our model. Bilanin also studied the evaporation of the particles near the surface of the airfoil and concluded that the evaporation does not have effect on the aerodynamic efficiency of airfoil. The assumption of non-deforming, spherical droplets simplifies the analysis, but in actual raindrops will deform as they enter the airfoil boundary layer.

In our work two-phase flow approach to the low and comparatively high Reynolds number airfoils has been employed, scaling laws for rain particles are used for the scaled airfoils, adding more realistic rain behavior to the airfoil using SA and  $k-\varepsilon$  turbulence models. The simulation results are compared with the experimental results done earlier and they show good agreement.

## II. MODELING OF RAIN PARTICLES

In experimental or numerical simulation, we measure the intensity of rainfall in terms of Liquid Water Content (LWC) of the air. The relation between rainfall rate  $R$  (mm/h) to LWC ( $\text{g/m}^3$ ) for thunderstorm type rain is given by [20]

$$\text{LWC} = 0.054R^{0.84} \quad (1)$$

For light spread rain

$$\text{LWC} = 0.0889R^{0.84} \quad (2)$$

Subsequently we also need to measure the velocity of the particles striking the airplanes. The rain particles usually strike the airplane with terminal velocity at landing or take off. The terminal velocity of the raindrops is the function of the diameter of the particles and is given by Markowitz as [3].

$$V_T (\text{m/sec}) = 9.58 \left\{ 1 - \exp \left( - \frac{d (\text{mm})^{1.147}}{1.77} \right) \right\} \quad (3)$$

Where  $V_T$  is the terminal velocity (m/sec), and  $D$  is the rain droplet size in mm.

## III. SCALING OF RAIN EFFECTS

Because of the complexity of the two-phase flow environment the established wind tunnel and numerical simulation to full scale, scaling laws may not be applicable in real rain environment. In 1985, Bilanin [19] analysis showed that the variables like, density, kinematic viscosity, surface tension interaction, mean drop spacing, volumetric mean drop diameter and drop velocity of water are important scaling parameters for rain effects on airfoil aerodynamic efficiency. As we have used scaled model for the numerical simulation, so scaling laws given by ref [19] are used for small scale airfoil to compare result for the full scale airfoil wind tunnel test which are given by

$$\frac{N}{\rho_a U^2 c^2} = f(\pi_1, \dots, \pi_9) \quad (4)$$

Where  $N$  is aerodynamic force on the airfoil,  $\rho_a$  is air density,  $U$  is the flight speed and  $c$  is mean spacing between particle drops.

## IV. COMPUTATIONAL & GEOMETRIC MODELING

For our aerodynamic analysis in heavy rain we chose cambered NACA 64210 and symmetric NACA 0012 airfoils. In this research, we used gridgen software to create the geometry and generate the grid around airfoils. We solved conservation equations of mass, momentum and energy of the flow field after discretization with finite volume method. K- $\varepsilon$  (RNG) and SA turbulence models are chosen for our numerical study. For air the ideal gas model was used to include effects of compressibility and the Sutherland Law as the viscosity model. In the discretization schemes, the upwind schemes were used (second order) to reach the final solution. The governing equations are written as

$$\frac{\partial \rho}{\partial t} + \frac{\partial}{\partial x_i} (\rho u_i) = 0 \quad (5)$$

$$\begin{aligned} \frac{\partial}{\partial t} (\rho u_i) + \frac{\partial}{\partial x_j} (\rho u_i u_j) = & - \frac{\partial p}{\partial x_i} + \frac{\partial}{\partial x_j} \left[ \mu \left( \frac{\partial u_i}{\partial x_j} + \frac{\partial u_j}{\partial x_i} - \frac{2}{3} \delta_{ij} \frac{\partial u_k}{\partial x_k} \right) \right] \\ & + \frac{\partial}{\partial x_j} (-\rho \overline{u_i' u_j'}) \end{aligned} \quad (6)$$

Where  $-\rho \overline{u_i' u_j'}$  is the Reynolds stress term. The transport Equations of  $k$  and  $\varepsilon$  used in  $k-\varepsilon$  turbulence model are written as

$$\begin{aligned} \frac{\partial}{\partial t} (\rho k) + \frac{\partial}{\partial x_j} (\rho k u_j) = & \frac{\partial}{\partial x_j} \left( \alpha_k \mu_{\text{eff}} \frac{\partial k}{\partial x_j} \right) + \\ G_k + G_b - \rho \varepsilon - Y_M + S_k \end{aligned} \quad (7)$$

$$\frac{\partial}{\partial t}(\rho\varepsilon) + \frac{\partial}{\partial x_j}(\rho\varepsilon u_j) = \frac{\partial}{\partial x_j} \left( \alpha_k \mu_{eff} \frac{\partial k}{\partial x_j} \right) + C_{1\varepsilon} \frac{\varepsilon}{k}$$

$$(G_k + C_{3\varepsilon} Gb) - C_{2\varepsilon} \rho \frac{\varepsilon^2}{k} - R_\varepsilon + S_\varepsilon \quad (8)$$

Similarly for SA model the equation is written as

$$\frac{\partial}{\partial t}(\rho\tilde{v}) + \frac{\partial}{\partial x_i}(\rho\tilde{v}u_i) = G_v + \frac{1}{\sigma_v}$$

$$\left[ \frac{\partial}{\partial x_j} \left\{ (\mu + \rho\tilde{v}) \frac{\partial \tilde{v}}{\partial x_j} \right\} + C_{b2}\rho \left( \frac{\partial \tilde{v}}{\partial x_j} \right)^2 \right] - Y_v + S \quad (9)$$

For air, the ideal gas model was used to include the effects of compressibility and the Sutherland Law is used as the viscosity model. In the discretization schemes, the upwind schemes (second order) were used to reach the final solution.

## V. TWO PHASE MODELING

Due to recent developments in computational fluid mechanics we have found the basis for further insight in to the dynamics of multi-phase flow. Currently there are two approaches for numerical calculation in multi-phase flow. The Eulerian-Eulerian approach and Eulerian-Lagrangian approach. In the Euler-Euler approach, the different phases are treated mathematically as interpenetrating continua. In Eulerian-Lagrangian the fluid phase is treated as a continuum, while the dispersed phase is solved by tracking a large number of particles through the calculated flow field. The particles can exchange momentum, mass, and energy with the fluid phase. Then the fundamental assumption in the model is that the dispersed second phase occupies a low volume fraction, even though high mass loading  $\dot{m}_p > \dot{m}_f$  is acceptable.

The trajectories of discrete phase particles are computed by integrating the acceleration produced force balance on the particle, and is written in langrangian reference of frame. This force can be written [21-22] as

$$\frac{dv_p}{dt} = F_{Drag}(v - v_p) + F_x \quad (10)$$

Where  $F_x$  is an additional acceleration (force/unit particle mass term and  $F_{Drag}(v - v_p)$  is called the drag force per unit particle mass and is written as

$$F_{Drag} = \frac{18\mu C_D Re}{\rho_p d_p^2 24} \quad (11)$$

Here  $v$  is fluid phase velocity,  $v_p$  is the particle velocity,  $\mu$  is the molecular viscosity of the fluid,  $\rho$  is the fluid density,  $\rho_p$  is the density of the particle,  $d_p$  is the diameter of the particle and  $Re$  is the relative Reynolds number given by

$$Re = \frac{\rho d_p |v_p - v|}{\mu} \quad (12)$$

## VI. RELATIVELY HIGH REYNOLDS NUMBER NACA 64210 AIRFOIL SIMULATION & RESULTS

For relatively high Reynolds number case we chose NACA 64210 airfoil. We used Gridgen software as shown in fig. 1

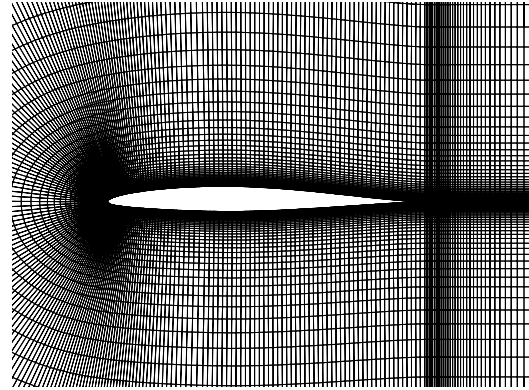


Fig. 1 Grid around Airfoil NACA 64210

Gridgen is very powerful software and can produce structured un-structured 2D and 3D meshes. In our case for NACA 64210 cambered airfoil, the chord length of airfoil is 1 m and number of cell 32856. The Reynolds number is set to  $3 \times 10^6$  to be consistent with the parameters of theory of wing section [23] and Wan [21]. We used Spalart-Allmaras and  $K-\varepsilon$  turbulence models for our studies of turbulent flow. In our analysis the lift and the drag coefficients agree well with the experiment before the stall angle of attack  $\alpha$ . Our results tendencies are similar to the experimental and numerical results done earlier. So according to previous simulation and our results, it can be stated that before stall angle simulation can provide good results that are consistent with the experimental results also.

In order to implement discrete phase modeling, first of all we have to construct rain injection. We have to establish the rain injection control volume for our case. For implementation of the DPM, we needed to input mass flow rate for each injection. For our case for cambered NACA 64210 airfoil with 1 m chord length we assumed that injection area is  $16 \times 1 m^2$ , calculated free stream velocity is 43 m/sec, thus we obtained volume flow rate of  $688 m^3/sec$ . For rain condition of  $LWC 39 g/m^3$ , according to volume flow rate calculated above the mass flow rate is 26.83 kg/sec. From previous research the distance between consecutive particles in heavy rain is 7 cm and as we are using scaled model of airfoil so rain particle distance is to be scaled also [19], so our scaled distance is 2.3 cm. similarly the rain particle diameter and terminal velocity is scaled. Thus we acquire 697 number of injection point of particles. Hence the mass flow rate of each particle stream is 0.038514 kg/sec. In our simulation we used  $LWC 0 g/m^3$ ,  $25 g/m^3$  and  $39 g/m^3$  rain rate cases to be consistent with Bezos experiment conditions. The results are compared with Bezo's results, Fig. 2-5 show lift

and drag coefficients for 3 rain rates. The decrease in lift and increase drag is successfully simulated for both SA and  $k-\epsilon$  turbulence models. With the increment of rain rate the decrement in aerodynamic efficiency is clearly shown. The lift decrease and drag increases with rain rate, and our numerical results agree well with the experimental tendencies. The L/D of our simulation and experiments done earlier are also more consistent with each other. Fig. 6 is clearly showing these tendencies.

The L/D degradation ratio for simulation using SA model reaches up to 28% for AOA of 10 degree, which is very close to the experimental results. So the aerodynamic efficiency degrades more than one fourth of the original value for rain rate  $39 \text{ g/m}^3$  and for light rain  $25 \text{ g/m}^3$  degrades up to one fifth of the original value. Because of such a significant loss of aerodynamic efficiency due to heavy rain, the results are very important for airplane and UAVs designers, engineers and pilots.

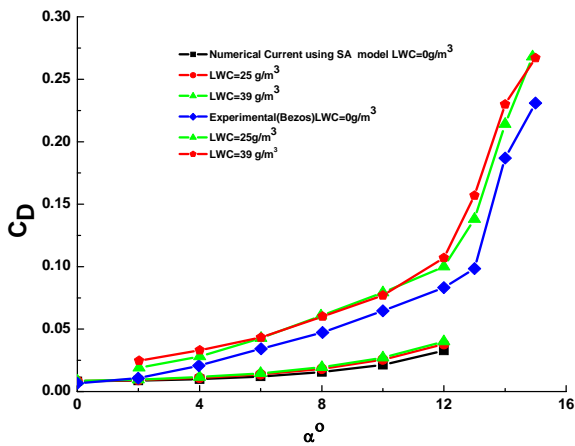


Fig. 2: CD VS AOA for Different Rain rates using SA Turbulence Model

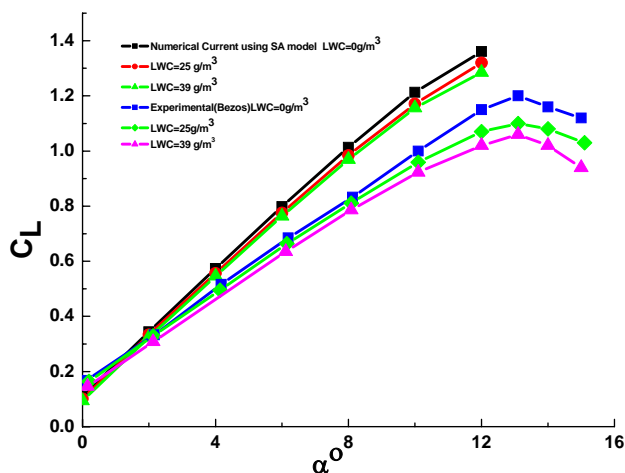


Fig. 3: CL VS AOA using SA Turbulence Model

In Fig. 7 particles are shown around airfoil 64210. We can see the water particles in 2D domain around the airfoil in fig. Particles wrapped around the airfoil NACA64210 on both upper and down side can clearly be seen. Particles are splashed back from the airfoil wall. These splashed particles from wall, the ejected fog of splashed particle and the thin water layer on the airfoil can be seen easily. They all contribute in increment of drag and decrement of lift of the airfoil.

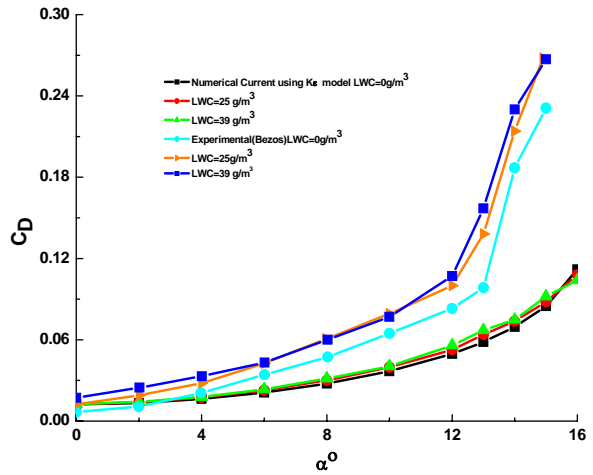


Fig. 4: CD VS AOA for Different Rain rates using  $K-\epsilon$  Turbulence Model

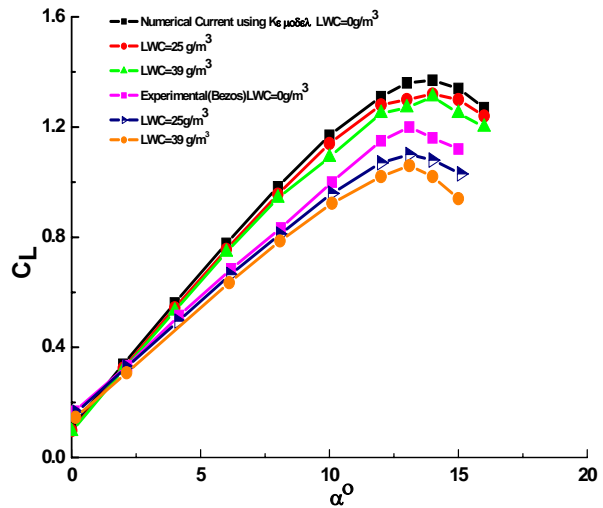


Fig. 5: CL VS AOA using  $K-\epsilon$  Turbulence Model

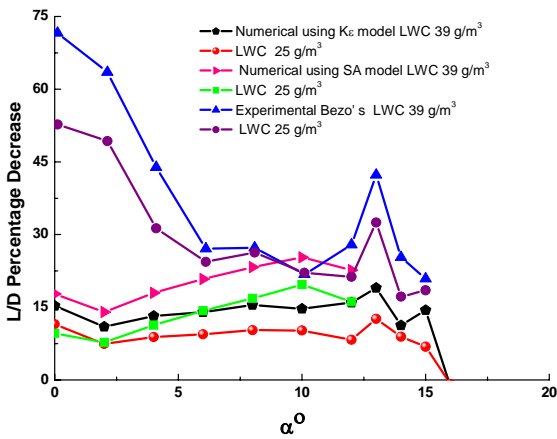


Fig. 6: L/D Percentage Degradation for Simulation and Experimental Results for Different Rain rates

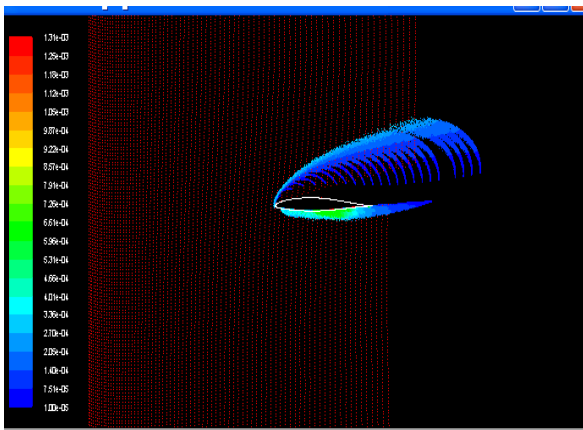


Fig. 7: Particle Tracks around NACA 64210

VII. LOW REYNOLDS NUMBER NACA 0012 AIRFOIL SIMULATION & RESULTS

For low Reynolds number case we chose symmetric airfoil NACA 0012. The grid is shown in Fig. 8. The chord length is 0.14 m and number of cell is 49306. The Reynolds number is set to  $3.1 \times 10^5$  to be consistent with Hansman [12] experiment.

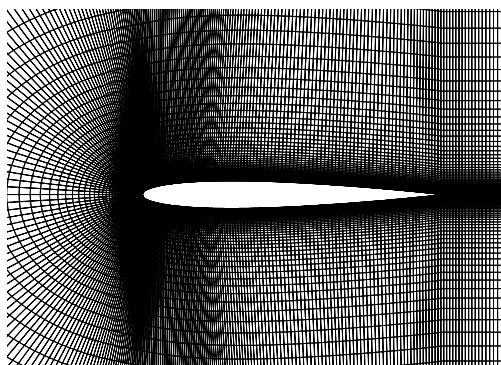


Fig. 8: Grid around Airfoil NACA 0012

For our low Reynolds number case for symmetric NACA0012 airfoil, we used Spalart-Allmaras and  $k-\epsilon$  turbulence models. Our numerical results agrees well with the experimental results done by Hansman before the stall angle.

For our case we assumed, the injection area to be  $2.5 \times 1 m^2$  and free stream velocity 31.3 m/sec, thus obtaining volume flow rate of  $78.25 m^3/sec$ . For rain condition of  $LWC 39 g/m^3$ , according to volume flow rate calculated above the mass flow rate is 3.05 kg/sec. Scaled particle distance is 0.98 cm. The rain particle diameter 0.56mm and terminal velocity 2.25 m/sec is chosen for the simulation. Thus we acquire 255 number of injection point of particles. Hence the mass flow rate of each particle stream is 0.011963 kg/sec. In our simulation we used  $LWC 0 g/m^3, 30 g/m^3$  and  $39 g/m^3$  rain rate cases. The results are compared with Hansman [12] wind tunnel experiment results. Fig. 9-10 show lift and drag coefficients for 3 rain rates for SA turbulence model, while Fig. 11-12 show lift and drag coefficients for 3 rain rates for  $K-\epsilon$  turbulence model. The lift degradation and drag increment is successfully simulated for both SA and  $K-\epsilon$  model. It can be seen from figures that for NACA 0012 airfoil the lift and drag in rain environment is not a function of LWC, while for NACA 64210 LWC greatly affects the lift and drag coefficients. For NACA 0012 SA turbulence model the results are much closer to the experimental results as the SA model is low Reynolds number model, requiring the viscous-affected region of the boundary layer to be properly resolved.

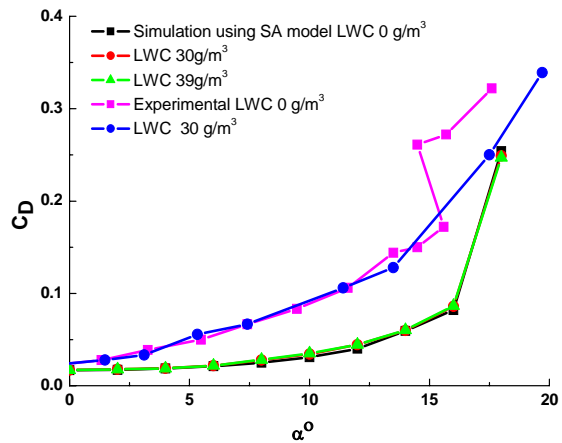


Fig. 9: CD vs. AOA for Different Rain rates using SA Turbulence Model

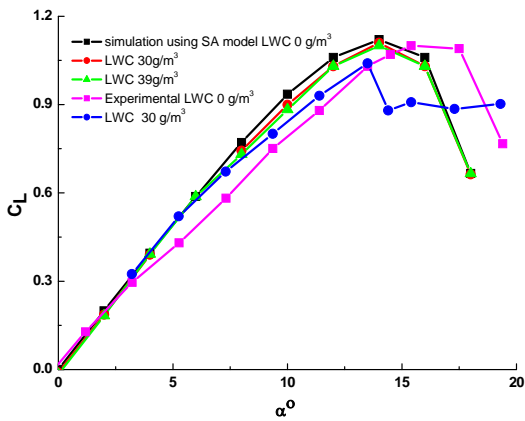


Fig. 10: CL vs. AOA using SA Turbulence Model

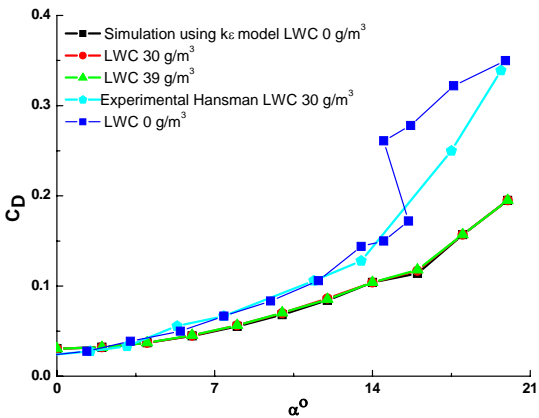


Fig. 11: CD vs. AOA  $K - \epsilon$  Turbulence Model

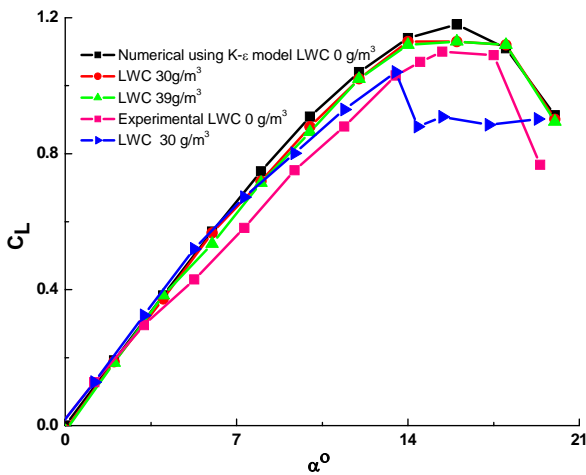


Fig. 12: CL vs. AOA using  $K - \epsilon$  Turbulence Model

It can also be seen that the L/D of simulation and experiments are more consistent. Fig. 13 is clearly showing these tendencies.

The L/D degradation ratio for simulation using SA model reaches up to 20% for AOA 10 degree, which is very close to the experimental results. So the aerodynamic efficiency degrades more than one sixth of the original value in rain environment.

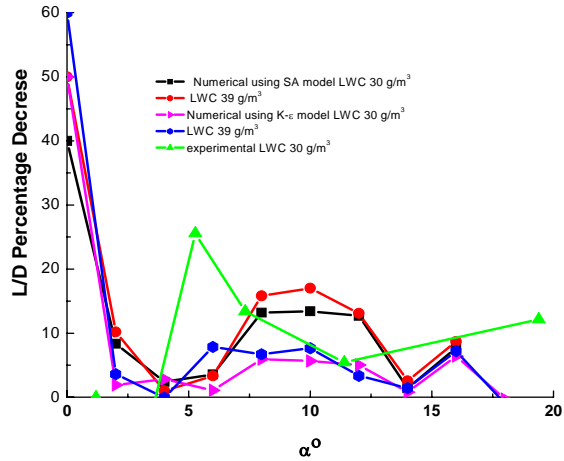


Fig. 13: L/D Percentage Decrease vs. AOA

In Fig. 14 particles are shown around airfoil 64210. We can see the water particles in 2D domain around the airfoil in fig. Particles wrapped around the airfoil NACA0012 on both upper and down side can clearly be seen. Particles are splashed back from the airfoil wall. These splashed particles from wall, the ejecta fog of splashed particle and the thin water layer on the airfoil can be seen easily. They all contribute in increment of drag and decrement of lift of the airfoil.

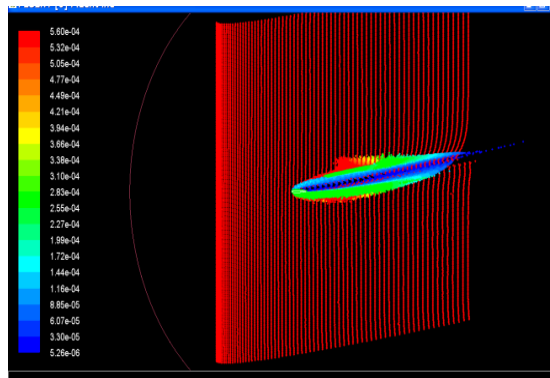


Fig. 14: Particles Tracks around NACA 0012

In fig. 15-18 the pressure distribution around the NACA 64210 NACA 0012 are shown for LWC 0, 39g/m³. Clearly it can be seen from figures that the Pressure difference between upper and lower surface of airfoils leading edge decreases with rain for both airfoils, so the lift and L/D ratio of airfoils decrease with rain.



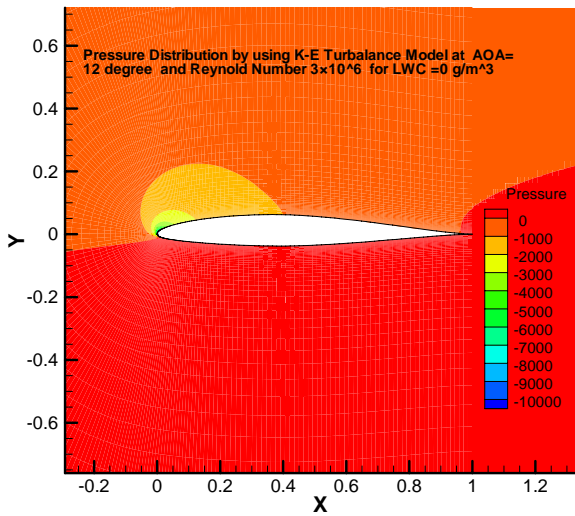


Fig. 15: Pressure Distribution around NACA 64210 LWC 0 g/m<sup>3</sup>

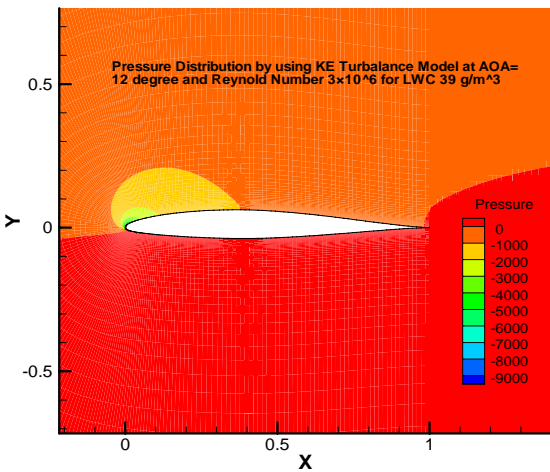


Fig. 16: Pressure Distribution around NACA 64210 LWC 39 g/m<sup>3</sup>

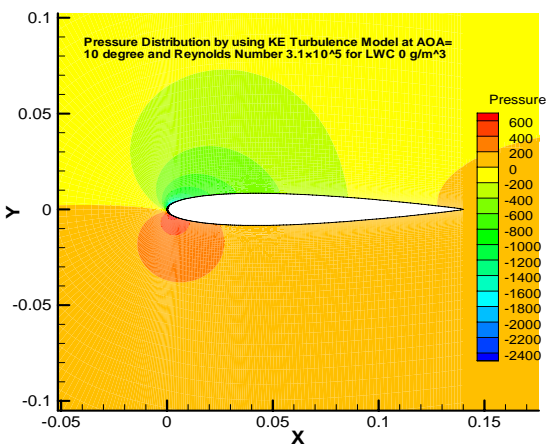


Fig. 17: Pressure Distribution around NACA 0012 LWC 0 g/m<sup>3</sup>

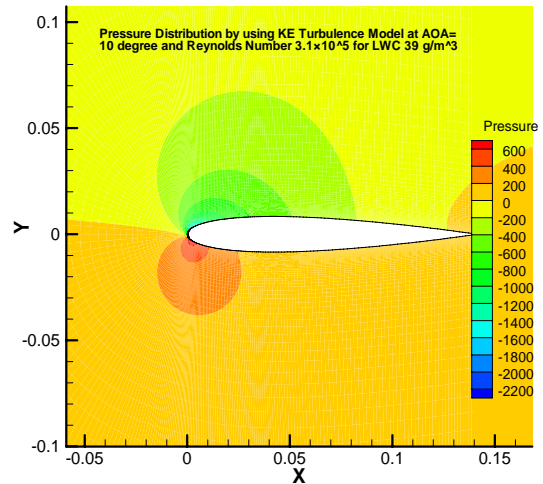


Fig. 18: Pressure Distribution around NACA 0012 LWC 39 g/m<sup>3</sup>

VIII. CONCLUSION

In summary we used two phase flow scheme to include effects of heavy rain on aerodynamic efficiency of 2-D airfoils. The degradation in the aerodynamic efficiency have been predicted in our simulation results. For our case we selected cambered NACA 64210 (relatively high Reynolds number) and symmetric NACA 0012 (Low Reynolds number case). For scaled models of our airfoils we employed discrete phase (DPM). Our numerical results show aerodynamic efficiency loss for both the airfoils and also consistent with the experimental work done before stall angle.

The experimental data of the heavy rain effect on aircraft is not much available, because the experimentation to include rain effects is very difficult, and expensive to conduct, so it is easy and better to simulate numerically the rain effects on different kinds of airfoils and wings. For NACA 64210 for Reynolds number  $3 \times 10^6$ , the L/D degradation reaches up to 28% for AOA 10°. This is a big loss in aerodynamic efficiency, so in future the designer of airplanes and UAVs must consider these facts while designing their airplanes and UAVs. For NACA 64210 airfoil the lift and drag coefficients of numerical simulation agrees well with the experimental results. The L/D degradation in average shows more consistency with the experiment. For NACA 0012 for Reynolds number  $3.1 \times 10^5$ , the effect of heavy rain is less than NACA 64210 Reynolds number  $3 \times 10^6$ . But results are still important when considering low Reynolds number vehicles such as mini-RPVs and sailplanes.

It is also seen from simulation and experimental results that for NACA 64210 the aerodynamic efficiency in rain environment is function of LWC while for NACA 0012 LWC value does not have much effect on aerodynamic efficiency in heavy rain environment.

Finally the numerical results are very good in agreement with the experimental results and can be important for future airplane and UAVs designs to fly in severe weather conditions and for aviation pilots to control and maneuver the airplanes better.

## REFERENCES

- [1] Haines, P. A. and Luers, J. K., "Aerodynamic Penalties of Heavy Rain on Landing Aircraft," *Journal of Aircraft*, Vol. 20, No. 2, February 1983, pp. 111-119.
- [2] Joss, J and Waldvogal, A., "Raindrop Size Distribution and Sampling Size Error," *J. Atmos. Sci.*, Vol. 26, no.3, May 1969, pp. 566-569.
- [3] Markowitz, A. M., "Raindrop Size Distribution Expression," *Journal of Applied Meteorology*, Vol. 15, 1976, pp. 1029-1031.
- [4] Rhode, R. V., "Some Effects of Rain fall on Flight of Airplanes and on Instrument Indications," NACA TN903, April 1941.
- [5] Haines, P. A. and Luers, J. K., "Experimental Measurement of Rain Effects Aircraft aerodynamics," AIAA, paper 83-0275, January 1983.
- [6] Luers, J. K., "heavy Rain effects on aircrafts" AIAA, paper 83-0206, jan, 1983.
- [7] Luers, J. K. and Haines, P. A., "heavy Rain Influence on Airplane Accidents" *Journal of Aircraft*, Vol. 20, No. 2, February 1983, pp. 187-191.
- [8] Valentine, J. R., "Airfoil Performance in Heavy Rain" *Transportation Research Record*, No. 1428, January 1994, pp.26-35
- [9] Valentine, J. R. and Decker, R. A., "Tracking of Raindrops in flow over an airfoil" *Journal of Aircraft*, Vol. 32, No. 1, February 1983, pp. 100-105
- [10] Valentine, J. R. and Decker, R. A., "A Lagrangian-Eulerian Scheme for Flow Around an Airfoil in Rain," *Int. J. Multiphase Flow*, Vol. 32, No. 1, 1995, pp. 639-648.
- [11] Wan T. and Wu S. W., "Aerodynamic Analysis under Influence of Heavy Rain," *Journal of Aeronautics, Astronautics and Aviation*, Vol. 41, No. 3, September 2009, pp.173-180.
- [12] Hansman, R. J. Jr. and Craig, A. P., "Low Reynolds Number Tests of NACA 642-10, NACA 0012, and Wortmann FS67-K170 Airfoils in Rain" *Journal of Aircraft*, Vol. 24, No. 8, August 1987.
- [13] Thompson, B.E., Jang, J., and Dion, J. L., "Wing Performance in Moderate Rain," *Journal of Aircraft*, Vol. 32, No. 5, Sep-Oct 1995, pp. 1034-1039.
- [14] Thompson, B.E. and Jang, J., "Aerodynamic Efficiency of wings in Rain," *Journal of Aircraft*, Vol. 33, No. 6, Nov-Dec 1996, pp. 1047-1053
- [15] Hating, E. C. Jr. and Manual, G. S., "Scale-Model Tests of Airfoils in Simulated Heavy Rain," *Journal of Aircraft*, Vol. 22, No. 6, June 1985, pp. 536-540.
- [16] . Abbot, I. H. and von Doenhoff, A. E., *Theory of Wing Section: Including a summary of Airfoil Data*, Dover Publication, New York, 1959.
- [17] Dunham, R. E. Jr., "The Potential Influence of Rain on Airfoil Performance" von Kamran Institute for Fluid Dynamics, 1987.
- [18] Carlse, W., and Hankey, W. L., "Numerical Analysis of Rain," AIAA Report, Jan 1984, 84-539
- [19] Bilanin, A. J., "Scaling Laws for Testing Airfoils under Heavy Rainfall," *Journal of Aircraft*, Vol. 24, No. 1, Jan. 1987, pp. 31-37.
- [20] Bezos, G. M., Dunham, R. E., Dunham, R. E. jr., Garl, jr., and Melson, W. E. Jr., "Wind Tunnel Aerodynamic Characteristics of a Transport-Type Airfoil in a Simulated Heavy Rain Environment ," NASA TM-3184, August 1992.
- [21] Wan T. and Pan S. P., "Aerodynamic Efficiency Study under the Influence of Heavy Rain via Two-Phase Flow Approach," 27<sup>th</sup> *International Congress of the Aeronautical Sciences*, 19-24 September 2010.
- [22] Fluent's User Guide.
- [23] Bezos, G. M. and Campbell, B. A., "Development of a Large-Scale, Outdoor, Ground-Based Test Capability for Evaluating the Effect of Rain on Airfoil," NASA TM-4420, April 1993.